New Inorganic/Organic Coordination Polymers Generated from Bidentate Schiff-Base Ligands

Yu-Bin Dong, Mark D. Smith, and Hans-Conrad zur Loye*

Department of Chemistry and Biochemistry, University of South Carolina, Columbia, South Carolina 29208

Received June 15, 2000

The coordination chemistry of the long conjugated bidentate Schiff-base ligands 1,4-bis(3-pyridyl)-2,3-diaza-1,3-butadiene (L1) and 2,5-bis(3-pyridyl)-3,4-diaza-2,4-hexadiene (L2) with cadmium and cobalt nitrate hydrates is investigated. Four new coordination polymers are prepared by solution reactions and fully characterized by infrared spectroscopy, elemental analysis, thermogravimetric analysis, and single-crystal X-ray diffraction. $[Cd(NO_3)_2(L1)_{1.5}\cdot 0.5(L1)]_n$ (**1**; monoclinic, $P2_1/c$; $a = 7.7729(16)$ Å, $b = 19.049(4)$ Å, $c = 17.865(4)$ Å, $\beta = 93.13(3)°$, $Z = 4$) is obtained by combination of L1 with $Cd(NO_3)_2\cdot 4H_2O$ in a benzene/methanol or THF/methanol mixed-solvent system. The structure features two-dimensional brick wall sheets that are cross-linked by weak noncovalent $\pi-\pi$ interactions (alternating face-to-face stacking of coordinated and uncoordinated L1 molecules) to generate a novel three-dimensional network. $[Co(NO_3)_2(L1)_{1.5}\cdot H_2O]_n$ (**2**; orthorhombic, *Ccca*; $a = 19.031(4)$ Å, $b = 33.627(7)$ Å, $c = 14.299(3)$ Å, $Z = 4$) is generated from the reaction of L1 with $Co(NO_3)_2\cdot 6H_2O$ in a benzene/ethanol mixed-solvent system. It forms with a unique three-dimensional framework that can be considered a new polymeric motif based on the 1:1.5 metal-to-ligand composition $M(L)_{1.5}$. The Cd(II) and Co(II) centers in **1** and **2**, which lie in seven-coordinate environments, generate two new types of building blocks. The topologies of these two new building blocks are distinctly different from the common "T-shaped" building block generated from the same $\{MN_3O_4\}$ coordination environment reported previously. $Cd(L2)_2(NO_3)_2$ (**3**) and $Co(L2)_2(NO_3)_2$ (**4**) are obtained by combination of L2 with $Cd(NO_3)_2\cdot 4H_2O$ and $Co(NO_3)_2\cdot 6H_2O$, respectively. Compounds **3** and **4** are isostructural, crystallizing in the monoclinic space group $P2_1/n$, with $a = 8.5802(17)$ Å, $b = 17.506(4)$ Å, $c = 10.443(2)$ Å, $\beta = 96.59(3)°$, and $Z = 2$ for **3** and $a = 8.5283(17)$ Å, $b = 17.408(4)$ Å, $c = 10.229(2)$ Å, $\beta = 97.05(3)°$, and $Z = 2$ for **4**. **3** and **4** adopt a novel one-dimensional chain structural motif, consisting of $M_2(L2)_2$ (M = Cd, Co) ringlike units. O···H−C hydrogen-bonding interactions in both **3** and **4** play a significant role in aligning the polymer strands in the solid state.

Introduction

Owing to their potential as new functional solid materials,[1−4] interest in self-assembled coordination polymers with specific network topologies has grown rapidly and has focused on structure building and the deliberate design of polymeric coordination compounds.[5−8] In principle, some control over network topology can be gained by judicious selection of reaction-influencing factors, such as the chemical structure of the organic spacers (ligands), the coordination geometry preference of the metal, the inorganic counterions, and the metal-to-ligand ratio.[9−12] So far, among the many diverse efforts to find

* To whom correspondence should be addressed. E-mail: zurloye@sc.edu.

(1) (a) Fujita, M.; Kwon, Y. J.; Washizu, S.; Ogura, K. *J. Am. Chem. Soc.* **1994**, *116*, 1151. (b) Lin, W.; Evans, O. R.; Xiong, R.-G.; Wang, Z. *J. Am. Chem. Soc.* **1998**, *120*, 13272.

(2) (a) Yaghi, D. M.; Li, H. *J. Am. Chem. Soc.* **1995**, *117*, 10401. (b) Yaghi, D. M.; Li, H.; Groy, T. L. *J. Am. Chem. Soc.* **1996**, *118*, 9096.

(3) (a) Garder, G. B.; Venkataraman, D.; Moore, J. S.; Lee, S. *Nature* **1995**, *374*, 792. (b) Garder, G. B.; Kiang, Y.-H.; Lee, S.; Asgaonkar, A.; Venkataraman, D. *J. Am. Chem. Soc.* **1996**, *118*, 6946.

(4) (a) Kahn, O.; Pei, Y.; Verdguer, M.; Renard, J. P.; Sletten, J. *J. Am. Chem. Soc.* **1988**, *110*, 782. (b) Inoue, K.; Hayamizu, T.; Iwamura, H.; Hashizume, D.; Ohashi, Y. *J. Am. Chem. Soc.* **1996**, *118*, 1803. (c) Tamaki, H.; Zhong, Z. J.; Matsumoto, N.; Kida, S.; Koikawa, M.; Achiwa, N.; Hashimoto, Y.; Okawa, H. *J. Am. Chem. Soc.* **1992**, *114*, 6974.

(5) Bein, T., Ed. *Supramolecular Architecture*: *Synthetic Control in Thin Films and Solids*; ACS Symposium Series 449; American Chemical Society: Washington, DC, 1992.

(6) Amabilino, D. B.; Stoddart, J. F. *Chem. Rev.* **1995**, *95*, 2725.

(7) Herrman, W. A.; Huber, N. W.; Runte, O. *Angew. Chem., Int. Ed. Engl.* **1995**, *34*, 2187.

(8) Stein, A.; Keller, S. W.; Mallouk, T. E. *Science* **1993**, *259*, 1558.

(9) (a) Kuroda-Sowa, T.; Horrino, T.; Yamamoto, M.; Ohno, Y.; Maekawa, M.; Munakata, M. *Inorg. Chem.* **1997**, *36*, 6382. (b) Munakata, M.; Wu, L. P.; Kuroda-Sowa, T. *Bull. Chem. Soc. Jpn.* **1997**, *70*, 1727. (c) Munakata, M.; Wu, L. P.; Kuroda-Sowa, T.; Maekawa, M.; Moriwaki, K.; Kitagawa, S. *Inorg. Chem.* **1997**, *36*, 5416. (d) Hennigar, T. L.; MacQuarrie, D. C.; Losier, P.; Rogers, R. D.; Zaworotko, M. J. *Angew. Chem., Int. Ed. Engl.* **1997**, *36*, 972. (e) Lloret, F.; Munno, G. D.; Julve, M.; Cano, J.; Ruiz, R.; Caneschi, A. *Angew. Chem., Int. Ed. Engl.* **1998**, *37*, 135.

(10) (a) Lu, J.; Paliwala, T.; Lim, S. C.; Yu, C.; Niu, T.; Jacobson, A. J. *Inorg. Chem.* **1997**, *36*, 923. (b) Munakata, M.; Ning, G. L.; Kuroda-Sowa, T.; Maekawa, M.; Suenaga, Y.; Harino, T. *Inorg. Chem.* **1998**, *37*, 5651. (c) Power, K. N.; Hennigar, T. L.; Zaworotko, M. J. *New J. Chem.* **1998**, *22*, 177. (d) Jung, O. S.; Park, S. H.; Kim, K. M.; Jang, H. G. *Inorg. Chem.* **1998**, *37*, 5781. (e) Losier, P.; Zaworotko, M. J. *Angew. Chem., Int. Ed. Engl.* **1996**, *35*, 2779. (f) Gudbjartson, H.; Biradha, K.; Poirier, K. M.; Zaworotko, M. J. *J. Am. Chem. Soc.* **1999**, *121*, 2599. (g) Carlucci, L.; Ciani, G.; Proserpio, M. *J. Chem. Soc., Dalton Trans.* **1999**, 1799. (h) Furusho, Y.; Aida, T. *J. Chem. Soc., Chem. Commun.* **1997**, 2205.

(11) (a) Gable, R. W.; Hoskins, B. F.; Robson, R. *J. Chem. Soc., Chem. Commun.* **1990**, 1677. (b) Fujita, M.; Kwon, Y. J.; Sasaki, O.; Yamaguchi, K. *J. Am. Chem. Soc.* **1995**, *117*, 7287. (c) Robson, R.; Abrahams, B. F.; Batten, S. R.; Gable, R. W.; Hoskins, B. F.; Liu, J. In *Supramolecular Architecture*: *Synthetic Control in Thin Films and Solids*; Bein, T., Ed.; ACS Symposium Series 449; American Chemical Society: Washington, DC, 1992; Chapter 19. (d) Carlucci, L.; Ciani, G.; Proserpio, D. M.; Sironi, A. *J. Chem. Soc., Chem. Commun.* **1994**, 2755.

10.1021/ic0006504 CCC: $19.00
Published on Web 09/27/2000

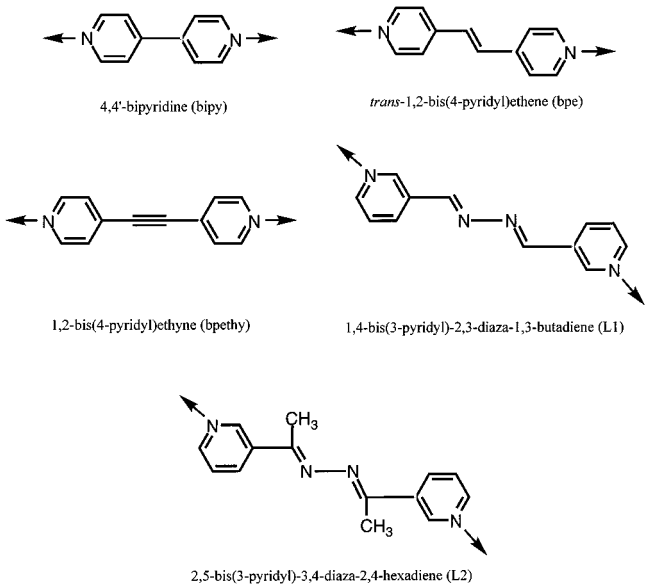

Figure 1. Rigid organic bipyridyl-based ligands used in the construction of coordination polymer frameworks.

key factors in the development of extended structures, the dominant synthetic strategy has been to select different organic ligands. During the past few years, many one-, two-, and three-dimensional coordination polymers have been generated from transition metal templates with rigid and flexible pyridyl-containing bidentate or multidentate organic spacers. Two excellent reviews by Zubieta and Schröder summarize some of these.[12] Up to now, however, except for the donor sites, most organic spacers employed in constructing coordination polymers do not contain free organic functional groups such as −OH, −COOH, −CHO, $-CONH_2$, −CR═N−, and −C≡N, which can play central roles in generating practical materials. The organic functional groups mentioned above have been shown to be very important for molecular-based photonic, electronic, and ionic devices.[13]

We have been exploring the rational design and synthesis of novel and functional coordination polymers based on N,N′-bidentate ligands, such as 4,4′-bipyridine (bipy), *trans*-1,2-bis-(4-pyridyl)ethene (bpe), and 1,2-bis(4-pyridyl)ethyne (bpethy) (Figure 1), and have reported several Co(II)-, Cd(II)-, and Cu(II)-based organic/inorganic polymers.[14] Very recently, we designed and synthesized a new type of long conjugated Schiff-base ligand, namely, 1,4-bis(3-pyridyl)-2,3-diaza-1,3-butadiene (L1).[14e] The specific geometry of this ligand, including the different relative orientations of N-donors and the zigzag conformation of the spacer moiety (−CR═N−N═CR−) between the two pyridyl groups (Figure 1), may result in coordination polymers with novel network patterns not achievable by other rigid linking ligands, such as bipy, bpe, and bpethy. Moreover, the −CR═N−N═CR− functional group in this type of ligand can potentially form hydrogen bonds (acting as acceptors) with donor groups to generate supramolecular systems with interesting host−guest chemistry.[14e] In addition, the −CR═N−N═CR− linking unit can also be considered a hydrogen bond donor precursor, with the change from hydrogen bond acceptor to hydrogen bond donor achieved easily by a reduction reaction. Herein, we wish to report the synthesis of a new member of this Schiff-base ligand family, namely, 2,5-bis(3-pyridyl)-3,4-diaza-2,4-hexadiene (L2), and the single-crystal structures of four polymeric coordination complexes, namely, $[Cd(NO_3)_2(L1)_{1.5}\cdot 0.5(L1)]_n$ (**1**), $[Co(NO_3)_2(L1)_{1.5}\cdot H_2O]_n$ (**2**), $Cd(L2)_2(NO_3)_2$ (**3**), and $Co(L2)_2(NO_3)_2$ (**4**), based on the two Schiff-base ligands L1 and L2.

Experimental Section

Materials and Methods. $Cd(NO_3)_2\cdot 4H_2O$ (Aldrich), $Co(NO_3)_2\cdot 6H_2O$ (Aldrich), 3-acetylpyridine (Aldrich), and hydrazine (35 wt % solution in water; Aldrich) were used as obtained, without further purification. The preparation and single-crystal structure of 1,4-bis(3-pyridyl)-2,3-diaza-1,3-butadiene has been published elsewhere.[14e] Infrared (IR) samples were prepared as KBr pellets, and spectra were obtained in the 4000−400 cm^{-1} range using a Perkin-Elmer 1600 FTIR spectrometer. ^1H NMR spectra were recorded using a 400 MHz Varian U400 spectrometer; chemical shifts are reported in δ relative to TMS. Thermogravimetric analyses were carried out using a TA Instrument SDT 2960 DTA−TGA apparatus in a flowing helium atmosphere at a heating rate of 10 °C/min. Elemental analyses were performed by the National Chemical Consulting Co.

Preparation of 2,5-Bis(3-pyridyl)-3,4-diaza-2,4-hexadiene (L2). 3-Acetylpyridine (2.43 mL, 22 mmol) was dissolved in ethanol (15 mL), followed by dropwise addition of the hydrazine solution (35 wt % solution in water, 1 mL, 11 mmol) in ethanol (8 mL). After the addition of two drops of formic acid, the mixture was refluxed for 5 h. The solvent was removed under vacuum, and the residue was extracted with methylene chloride and washed with water several times. The organic phase was dried over $MgSO_4$ and filtered, and upon removal of the solvent, an analytically pure bright yellow crystalline solid was obtained in 85% yield. ^1H NMR ($CDCl_3$, ppm): 9.15 (s, 2 H, pyridyl), 8.65 (d, 2 H, pyridyl), 8.21 (d, 2 H, pyridyl), 7.35 (m, 2 H, pyridyl), 2.29 (s, 6 H, $-CH_3$). IR (KBr, cm^{-1}): 1642 (m), 1606 (s), 1564 (s), 1536 (w), 1482 (s), 1412 (s), 1368 (s), 1293 (s). Anal. Calcd for $C_{14}H_{14}N_4$: C, 70.59; H, 5.88; N, 23.53. Found: C, 70.42; H, 5.78; N, 23.16.

Preparation of $Cd(L1)_{1.5}\cdot 0.5(L1)(NO_3)_2$ (1). A methanol solution (10 mL) of $Cd(NO_3)_2\cdot 4H_2O$ (92 mg, 0.30 mmol) was allowed to diffuse slowly into a benzene solution (10 mL) of L1 (126 mg, 0.60 mmol). Yellow crystals formed in ∼1 month. The yield was 70%. Compound **1** was also be prepared by diffusion of an ethanol solution of $Cd(NO_3)_2\cdot 4H_2O$ into a THF solution of L1, in 80% yield. IR (cm^{-1}, KBr pellet): 1630 (s), 1589 (m), 1558 (m), 1487 (s), 1385 (s), 1310 (s), 1228 (m), 1189 (s), 1120 (m), 1092 (w), 1051 (w), 1028 (s), 969 (s), 950 (w), 869 (s), 852 (s), 808 (s), 693 (s), 642 (s). Anal. Calcd for $C_{24}H_{20}N_{10}O_6Cd$: C, 43.88; H, 3.05; N, 21.33. Found: C, 43.67; H, 3.00; N, 21.16.

Preparation of $Co(L1)_{1.5}(NO_3)_2\cdot H_2O$ (2). A solution of $Co(NO_3)_2\cdot 6H_2O$ (82 mg, 0.30 mmol) in ethanol (10 mL) was allowed to diffuse slowly into a benzene solution (12 mL) of L1 (126 mg, 0.60 mmol). Deep red crystals formed in ∼1 month. The yield was 85%. IR (cm^{-1}, KBr pellet): 1634 (s), 1604 (s), 1576 (m), 1471 (s), 1417 (s), 1298 (s), 1191 (s), 1128 (s), 1102 (s), 1054 (s), 1032 (s), 984 (s), 966 (s), 944 (w), 880 (s), 825 (m), 810 (s), 739 (m), 702 (s), 640 (s). Anal. Calcd for $C_{18}H_{15}N_8O_6Co\cdot H_2O$: C, 41.87; H, 3.30; N, 21.71. Found: C, 41.54; H, 3.27; N, 21.56.

Preparation of $Cd(L2)_2(NO_3)_2$ (3). A colorless solution of $Cd(NO_3)_2\cdot 4H_2O$ (76 mg, 0.25 mmol) in methanol (5 mL) was carefully layered onto a solution of L2 (126 mg, 0.50 mmol) in THF. Diffusion between the two phases over a period of 1 week produced colorless multifaceted crystals in 90% yield. Compound **3** was also be obtained

(12) (a) Blake, A. J.; Champness, N. R.; Hubberstey, P.; Li, W.-S.; Withersby, M. A.; Schröder, M. *Coord. Chem. Rev.* **1999**, *183*, 117. (b) Hagrman, P. J.; Hagrman, D.; Zubieta, J. *Angew. Chem., Int. Ed. Engl.* **1999**, *38*, 2638.

(13) (a) Lehn, J.-M. *Angew. Chem., Int. Ed. Engl.* **1990**, *29*, 1304. (b) Lehn, J.-M. *Angew. Chem., Int. Ed. Engl.* **1988**, *27*, 89.

(14) (a) Dong, Y.-B.; Layland, R. C.; Smith, M. D.; Pschirer, N. G.; Bunz, U. H. F.; zur Loye, H.-C. *Inorg. Chem.* **1999**, *38*, 3056. (b) Dong, Y.-B.; Layland, R. C.; Pschirer, N. G.; Smith, M. D.; Bunz, U. H. F.; zur Loye, H.-C. *Chem. Mater.* **1999**, *11*, 1415. (c) Dong, Y.-B.; Smith, M. D.; Layland, R. C.; zur Loye, H.-C. *Inorg. Chem.* **1999**, *38*, 5027. (d) Dong, Y.-B.; Smith, M. D.; Layland, R. C.; zur Loye, H.-C. *J. Chem. Soc., Dalton Trans.* **2000**, 775. (e) Dong, Y.-B.; Smith, M. D.; Layland, R. C.; zur Loye, H.-C. *Chem. Mater.* **2000**, *12*, 1156. (f) Dong, Y.-B.; Smith, M. D.; Layland, R. C.; zur Loye, H.-C. Unpublished results.

Table 1. Crystallographic Data for **1** and **2**

	1	**2**
formula	$C_{24}H_{20}CdN_{10}O_6$	$C_{18}H_{17}CoN_8O_7$
fw	656.90	516.33
crystal system	monoclinic	orthorhombic
a (Å)	7.7729(16)	19.031(4)
b (Å)	19.049(4)	33.627(7)
c (Å)	17.865(4)	14.299(3)
α (deg)	90	90
β (deg)	93.13(3)	90
γ (deg)	90	90
V (Å^3)	2641.2(9)	9151(3)
space group	$P2_1/c$	*Ccca*
Z value	4	4
ρ_{calcd} (g/cm^3)	1.652	1.447
μ(Mo Kα) (cm^{-1})	11.258	11.329
temp (°C)	23	23
no. of observns ($I > 3\sigma(I)$)	3493	3373
residuals:[a] R1; wR2	0.042; 0.106	0.063; 0.114

[a] $R1 = \Sigma||F_o| - |F_c||/\Sigma|F_o|$; $wR2 = [\Sigma[w(F_o^2 - F_c^2)^2/\Sigma w(F_o^2)^2]^{1/2}$. $GOF = [\Sigma w(F_o^2 - F_c^2)^2/(n - p)]^{1/2}$ (n = number of reflections; p = number of refined parameters). $w = 1/[\sigma^2(F_o^2) + (aP)^2 + bP]$, where P is $[2F_c^2 + \max(F_o^2, 0)]/3$.

Table 2. Crystallographic Data for **3** and **4**

	3	**4**
formula	$C_{28}H_{28}CdN_{10}O_6$	$C_{28}H_{28}CoN_{10}O_6$
fw	713.00	659.53
crystal system	monoclinic	monoclinic
a (Å)	8.5802(17)	8.5283(17)
b (Å)	17.506(4)	17.408(4)
c (Å)	10.443(2)	10.229(2)
α (deg)	90	90
β (deg)	96.59(3)	97.05(3)
γ (deg)	90	90
V (Å^3)	1558.1(5)	1507.1(5)
space group	$P2_1/n$	$P2_1/n$
Z value	2	2
ρ_{calcd} (g/cm^3)	1.520	1.453
μ(Mo Kα) (cm^{-1})	11.258	11.329
temp (°C)	23	23
no. of observns ($I > 3\sigma(I)$)	2423	2655
residuals:[a] R1; wR2	0.040; 0.093	0.050; 0.122

[a] $R1 = \Sigma||F_o| - |F_c||/\Sigma|F_o|$; $wR2 = [\Sigma w(F_o^2 - F_c^2)^2/\Sigma w(F_o^2)^2]^{1/2}$. $GOF = [\Sigma w(F_o^2 - F_c^2)^2/(n - p)]^{1/2}$ (n = number of reflections; p = number of refined parameters). $w = 1/[\sigma^2(F_o^2) + (aP)^2 + bP]$, where P is $[2F_c^2 + \max(F_o^2, 0)]/3$.

in a methylene chloride/methanol mixed-solvent system in the same yield. IR (KBr, cm^{-1}): 1614 (s), 1578 (s), 1454 (s), 1284 (s), 1200 (s), 1127 (s), 1092 (s), 1036 (s), 962 (s), 820 (s), 786 (s), 708 (s), 648 (s), 641 (s). Anal. Calcd for $C_{28}H_{28}N_{10}O_6Cd$: C, 47.16; H, 3.93; N, 19.65. Found: C, 47.06; H, 3.72; N, 19.36.

Preparation of Co(L2)$_2$(NO$_3$)$_2$ (4). An ethanol solution (10 mL) of $Co(NO_3)_2 \cdot 6H_2O$ (72 mg, 0.25 mmol) was allowed to diffuse into a THF solution (8 mL) of L2 (126 mg, 0.50 mmol) in a test tube for 2 weeks. The large deep red multifaceted crystals that formed at the ethanol/THF interface were collected by filtration. Yield: 83%. Compound **4** was also be obtained in a methylene chloride/methanol mixed-solvent system in the same yield. IR (KBr, cm^{-1}): 1614 (s), 1434 (s), 1284 (s), 1199 (s), 1093 (s), 1034 (s), 964 (s), 820 (s), 788 (s), 709 (s), 650 (s), 642 (s). Anal. Calcd for $C_{28}H_{28}N_{10}O_6Co$: C, 50.99; H, 4.25; N, 21.25. Found: C, 50.72; H, 4.15; N, 21.16.

Single-Crystal Structure Determination. Suitable single crystals of **1**−**4** were selected and epoxied in air onto thin glass fibers. Intensity measurements were made at 20 °C using a Rigaku AFC6S four-circle diffractometer equipped with Mo Kα radiation ($\lambda = 0.710\ 69$ Å). For each compound, the initial unit cell was determined from 15 reflections randomly located using the AFC6 automatic search, center, index, and least-squares routines. After data collection, each cell was refined using 25 high-angle reflections in the range $35° < 2\theta < 2\theta_{max}$. Three standard reflections measured every 150 reflections showed no significant decay during data collection for each crystal. All structures were solved and refined by a combination of direct methods and difference Fourier syntheses, using SHELXTL.[15] After the location and refinement of all non-hydrogen atoms with isotropic thermal parameters, an absorption correction (DIFABS)[16] was applied. Subsequently, all non-hydrogen atoms were refined with anisotropic displacement parameters. Framework hydrogen atoms were placed in the calculated positions and refined using a riding model. A water molecule disordered over three crystallographic sites was found in **2**, for which hydrogen atoms could not be reliably located or calculated. Crystal data, data collection parameters, and refinement statistics for **1** and **2** and for **3** and **4** are listed in Tables 1 and 2, respectively. Relevant interatomic bond distances and bond angles for **1**−**4** are collected in Tables 3−6.

Table 3. Interatomic Distances (Å) and Bond Angles (deg) with Esd's (in Parentheses) for **1**

Cd−N(1)	2.334(3)	Cd−N(2)	2.342(3)
Cd−N(3)	2.360(3)	Cd−O(1)	2.428(4)
Cd−O(3)	2.489(3)	Cd−O(4)	2.433(3)
Cd−O(6)	2.441(3)		
N(1)−Cd−N(2)	98.29(12)	N(1)−Cd−N(2)	97.18(11)
N(2)−Cd−N(3)	164.39(11)	N(1)−Cd−O(1)	86.04(11)
N(2)−Cd−O(1)	85.88(12)	N(3)−Cd−O(1)	93.08(12)
N(1)−Cd−O(4)	137.04(12)	N(2)−Cd−O(4)	84.80(12)
N(3)−Cd−O(4)	85.36(12)	O(1)−Cd−O(4)	136.82(10)
N(1)−Cd−O(6)	85.14(12)	N(2)−Cd−O(6)	94.34(12)
N(3)−Cd−O(6)	89.08(13)	O(1)−Cd−O(6)	171.11(11)
O(4)−Cd−O(6)	51.94(11)	N(1)−Cd−O(3)	137.24(11)
N(2)−Cd−O(3)	87.63(11)	N(3)−Cd−O(3)	79.54(11)
O(1)−Cd−O(3)	51.99(10)	O(4)−Cd−O(3)	85.54(11)
O(6)−Cd−O(3)	136.89(11)		

Table 4. Interatomic Distances (Å) and Bond Angles (deg) with Esd's (in Parentheses) for **2**

Co−N(1)	2.175(3)	Co−N(3)	2.146(3)
Co−N(5)	2.151(3)	Co−O(1)	2.264(3)
Co−O(3)	2.215(3)	Co−O(4)	2.176(3)
Co−O(5)	2.333(3)		
N(3)−Co−N(5)	175.64(11)	N(3)−Co−N(1)	93.13(11)
N(5)−Co−N(1)	89.61(11)	N(3)−Co−O(4)	87.35(10)
N(5)−Co−O(4)	89.41(11)	N(1)−Co−O(4)	87.00(10)
N(3)−Co−O(3)	90.15(11)	N(5)−Co−O(3)	89.98(11)
N(1)−Co−O(3)	139.26(12)	O(3)−Co−O(4)	133.72(11)
N(3)−Co−O(1)	98.97(11)	N(5)−Co−O(1)	84.73(11)
N(1)−Co−O(1)	83.11(10)	O(4)−Co−O(1)	168.52(10)
O(3)−Co−O(1)	56.31(11)	N(3)−Co−O(5)	81.78(11)
N(5)−Co−O(5)	93.98(11)	N(1)−Co−O(5)	142.49(11)
O(4)−Co−O(5)	55.76(10)	O(3)−Co−O(5)	78.14(12)
O(1)−Co−O(5)	134.40(11)		

Results and Discussion

Synthesis. The coordination polymers **1**−**4** were synthesized by solution reactions between the new ligands L1 and L2 and $Cd(NO)_3 \cdot 4H_2O$ and $Co(NO_3)_2 \cdot 6H_2O$. When a solution of L1 in the nonpolar solvent benzene was treated with $Cd(NO)_3 \cdot 4H_2O$ in methanol and $Co(NO_3)_2 \cdot 6H_2O$ in ethanol, respectively, in a metal-to-ligand molar ratio of 1:2, compounds **1** and **2** were obtained as polymeric compounds with a "brick wall" structural motif for **1** and a unique three-dimensional network for **2**. It is worth pointing out that the coordination chemistry of L1 with transition metal templates such as Cd(II) and Co(II) appears to be quite versatile, with the products primarily dependent on the choice of solvent system and largely independent of the metal-to-ligand mole ratio. For example, when the ligand solvent is changed from benzene to polar methylene chloride, the reactions

(15) *SHELXTL*, Version 5.1; Bruker AXS, Inc.: Madison, WI, 1997.
(16) Walker, N.; Stuart, D. *Acta Crystallogr.* **1986**, *A39*, 158.

Table 5. Interatomic Distances (Å) and Bond Angles (deg) with Esd's (in Parentheses) for **3**

Cd−N(1)	2.319(3)	Cd−N(4)	2.371(3)
Cd−O(1)	2.337(3)	C(1)−N(1)	1.340(4)
C(1)−C(2)	1.370(5)	N(2)−N(3)	1.393(4)
N(5)−O(3)	1.152(6)	N(5)−O(1)	1.227(4)
C(6)−N(2)	1.279(4)	N(5)−O(2)	1.215(5)
C(6)−C(7)	1.494(5)	C(8)−C(9)	1.493(5)
N(1)−Cd−N(1)	180	N(1)−Cd−O(1)*	94.53(11)
N(1)−Cd−O(1)	85.47(11)	N(1)−Cd−N(4)*	88.42(10)
N(1)−Cd−N(4)	91.58(10)	N(4)*−Cd−O(1)	92.08(12)
N(4)−Cd−N(4)*	180	N(1)−C(1)−C(2)	122.4(3)
C(4)−C(6)−C(7)	120.2(3)	N(2)−C(6)−C(7)	123.9(3)
C(6)−N(2)−N(3)	116.4(3)	C(9)−N(3)−N(2)	116.5(3)
C(2)−C(3)−C(4)	119.4(3)	O(3)−N(5)−O(1)	121.1(4)

Table 6. Interatomic Distances (Å) and Bond Angles (deg) with Esd's (in Parentheses) for **4**

Co−N(1)	2.147(2)	Co−N(4)	2.201(3)
Co−O(1)	2.159(3)	C(1)−N(1)	1.348(4)
C(1)−C(2)	1.370(4)	N(2)−N(3)	1.392(4)
N(5)−O(3)	1.179(5)	N(5)−O(1)	1.250(3)
C(6)−N(2)	1.280(4)	N(5)−O(2)	1.198(4)
C(6)−C(7)	1.496(4)	C(8)−C(9)	1.496(4)
N(1)−Co−N(1)*	180	N(1)−Co−O(1)*	93.92(9)
N(1)−Co−O(1)	86.08(9)	N(1)−Co−N(4)*	92.43(9)
N(1)−Co−N(4)	87.57(9)	N(4)*−Co−O(1)	88.95(9)
N(4)−Co−N(4)*	180	N(1)−C(1)−C(2)	122.6(3)
C(4)−C(6)−C(7)	120.0(3)	N(2)−C(6)−C(7)	124.0(3)
C(6)−N(2)−N(3)	116.8(2)	C(9)−N(3)−N(2)	116.5(3)
C(2)−C(3)−C(4)	119.1(3)	O(3)−N(5)−O(1)	120.9(3)

of L1 with $Cd(NO_3)_2 \cdot 4H_2O$ in methanol and with $Co(NO_3)_2 \cdot 6H_2O$ in ethanol with the same metal-to-ligand ratio yield, as the only products, $[M(NO_3)_2(L1)_{1.5} \cdot CH_2CL_2]_n$ (M = Cd, Co),[14e] which crystallize with novel two-dimensional noninterpenetrating polycyclohexane motifs distinctly different from the polymeric motifs found in compounds **1** and **2**. In other words, the proper selection of solvent system and template ions in the synthetic process is critical in directing the self-assembly of coordination polymers, an observation that has been borne out by many previous studies.[10] Compound **1** can also be obtained by combination of the L1 spacer in the polar solvent THF with $Cd(NO_3)_2 \cdot 4H_2O$ in methanol, but in higher yields. Unfortunately, we were not able to grow high-quality single crystals suitable for X-ray diffraction by slow diffusion of $Co(NO_3)_2 \cdot 6H_2O$ in ethanol or methanol with L1 in THF. Toluene and 1,4-dioxane were also tried, and again, however, only poor-quality crystals of both the cadmium and cobalt compounds were obtained. In principle, crystallization via slow diffusion depends delicately on the rate of diffusion, but so far, several attempts to vary the interdiffusion rate (i.e., adding a pure solvent buffer layer between the ligand and reactant layers) have failed.

The long rigid bidentate ligand 2,5-bis(3-pyridyl)-3,4-diaza-2,4-hexadiene (L2) was prepared in 85% yield by the Schiff-base condensation reaction of 3-acetylpyridine with hydrazine (35 wt % solution in water) in ethanol under reflux conditions. Elemental analysis and the ^{1}H NMR and IR spectra are consistent with the formulation of L2. Compared to that of L1, the solubility of L2 in common organic solvents is clearly enhanced after introducing the two methyl groups. For example, it is readily soluble in methylene chloride, chloroform, THF, 1,4-dioxane, toluene, and benzene at room temperature. More importantly, the steric presence of the two methyl groups dramatically changes the structure of the reaction products. Compounds **3** and **4**, which are distinctly different from **1** and **2**, are the only isolable products from the reactions of L2 with $Cd(NO_3)_2 \cdot 4H_2O$ and $Co(NO_3)_2 \cdot 6H_2O$ at metal-to-ligand ratios of 1:2 in various solvent systems, for example, methylene chloride/methanol or THF/methanol for **3** and methylene chloride/methanol or THF/ethanol for **4**.

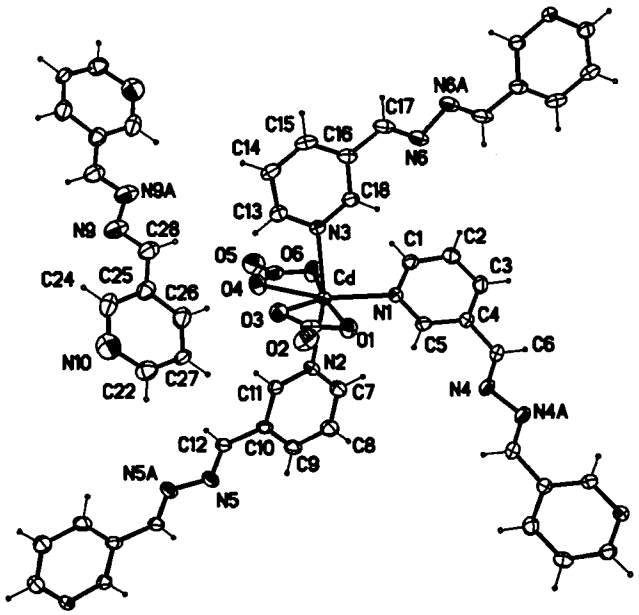

Figure 2. Distorted "T-shaped" environment at the cadmium center in **1**, drawn with 30% probability ellipsoids. The uncoordinated L1 ligand is also shown.

The new polymeric compounds reported here were isolated as bright yellow (**1**), deep-red (**2**), colorless (**3**), and red (**4**) crystals suitable for X-ray diffraction. Compounds **1**−**4** are insoluble in common organic solvents and in water, consistent with their polymeric natures. Crystals of **1**−**4** are air stable and retain their structural integrity at room temperature indefinitely. Besides single-crystal diffraction, **1**−**4** were characterized by IR spectroscopy, DTA-TGA, and elemental analyses, results of which were all consistent with the formulations of **1**−**4** obtained from the crystallography. The IR spectra[17] clearly indicated the presence of nitrate groups (1417−1200 cm^{-1}) in **1**−**4**. A strong splitting of the nitrate stretching bands was observed, demonstrating that the nitrate counterion entered the coordination sphere of Cd(II) and Co(II), again consistent with the single-crystal structure determinations.

Structural Analysis. 1. Building Blocks. (a) Of 1 and 2. As shown in Figures 2 and 3, the respective Cd(II) and Co(II) centers in **1** and **2** each lie in a heptacoordinate environment defined by three N-donors from three L1 ligands and four O-donors from two bidentate nitrate counterions. The uncoordinated L1 ligand found in **1** is also shown in Figure 2. For **1**, the Cd−N and Cd−O bond lengths range from 2.334(3) to 2.360(3) Å and from 2.428(4) to 2.489(3) Å (Table 3), respectively, typical for bond lengths in similarly coordinated compounds (e.g., $[Cd(NO_3)_2(4,4'\text{-bipy})_2] \cdot 2C_6H_4Br_2$,[1a] $[Cd(dpb)_{1.5}(NO_3)_2]$,[11b] and $[Cd(dpb)_{1.5}(NO_3)_2]$).[11b] In **2**, the Co−N and Co−O bond distances range from 2.146(3) to 2.175(3) Å and from 2.176(3) to 2.333(3) Å (Table 4), respectively, again consistent with corresponding bond lengths in, for example, $[Co(bipy)_{1.5}(NO_3)_2] \cdot 2CHCl_3$, $[Co(bipy)_{1.5}(NO_3)_2] \cdot MeCN$,[10e] [Co(1,4-bis(4-pyridyl)ethane)$_{1.5}$(NO$_3$)$_2$]·MeCN, and

(17) (a) Wang, Z.; Xiong, R.-G.; Foxman, B. M.; Wilson, S. R.; Lin, W. *Inorg. Chem.* **1999**, *38*, 1523. (b) Yaghi, D. M.; Li, H. *J. Am. Chem. Soc.* **1996**, *118*, 295.

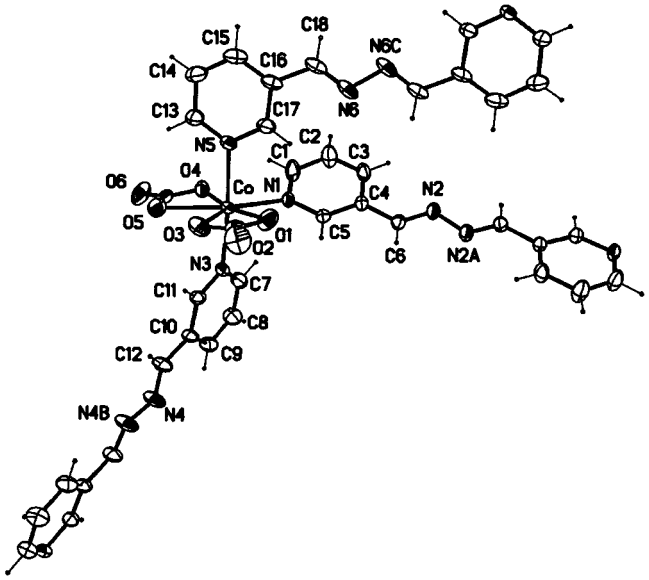

Figure 3. "F-shaped" environment at the cobalt center in **2**, drawn with 30% probability ellipsoids.

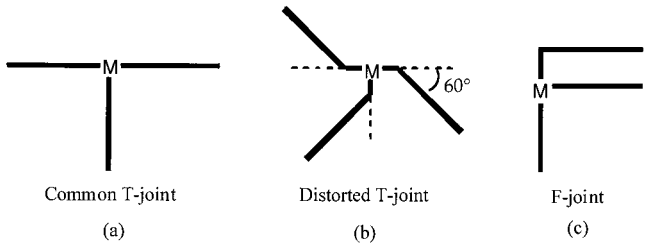

Figure 4. Schematic comparison of a common "T-joint", a distorted "T-joint", and an "F-joint".

$[Co(1,4\text{-bis}(4\text{-pyridyl})ethane)_{1.5}(NO_3)_2]\cdot 3CHCl_3$.[9d] However, the Co−O bond distances are significantly shorter than those in $[Co(bpethy)_{1.5}(NO_3)_2]\cdot MeOH$ (2.351−2.444 Å).[14b]

It is well-known that building blocks generated from $M(L)_{1.5}(NO_3)_2$ (L = rigid ligand; M = Cd, Co) subunits are typically of the "T-joint" variety (Figure 4a);[10c−f,14a−b] that is, the bond angles between the two neighboring M−N (M = Cd, Co) bonds are near 90° and the three rigid bidentate ligands extend outward from the metal center along the directions defined by the M−N (M = Cd, Co) bonds. The building blocks in both compounds **1** and **2**, however, are no longer common "T-joint" types, although the local N−M−N coordination bond angles (Tables 3 and 4) in both **1** and **2** are very close to typical "T-joint" bond angles. In **1**, the three coordinated L1 ligands do not extend outward along the three Cd−N bond directions but deviate clockwise by ca. 60° to form a distorted "T-shaped" building block (Figure 4b). In **2**, however, a surprisingly different orientation of the three coordinated L1 spacers is found. As shown in Figure 3, two of the three coordinated L1 ligands in **2** are oriented in almost the same direction, while the third extends almost perpendicularly to these. Such a building block can be described as a distorted "F-shaped" building block (Figure 4c). The two local structural motifs described here might be considered two new types of building blocks generated from the $M(L)_{1.5}(NO_3)_2$ (L = rigid ligand) composition. It is worth pointing out that, as indicated in Figures 2 and 3, the individual L1 ligands present in **1** and **2** are planar; i.e., the two pyridyl donor groups of each ligand are not rotated with respect to one another.

(b) Of 3 and 4. Compared to the cases of **1** and **2**, different coordination environments for Cd(II) and Co(II) are present in compounds **3** and **4**. As shown in Figure 5, the Cd(II) and Co(II) centers in **3** and **4**, which reside on crystallographic inversion centers, each feature a 4 + 2 pseudooctahedral $\{MN_4O_2\}$ coordination geometry with the equatorial sites occupied by four pyridyl nitrogen donors from L2; the axial positions are occupied by two monodentate nitrate counterions (for **3**, O(1)−Cd−O(1)* = 180°, O(1)−Cd−N(4)* = 87.92(12)°, N(1)−Cd−N(4) = 91.58(10)°, N(1)−Cd−N(1)* = 180°, and N(4)−Cd−N(4)* = 180°; for **4**, O(1)−Co−O(1)* = 180°, O(1)−Co−N(4)* = 91.05(9)°, N(1)−Co−N(4)* = 87.57(9)°, N(4)−Co−N(4)* = 180°, and N(1)−Co−N(1)* = 180°). The Cd−N (2.319(3)−2.371(3) Å) and Cd−O (2.337(3) Å) bond distances in **3** are very close to the corresponding bond lengths found in $[Cd(NO_3)_2(4,4'\text{-bipy})_2]\cdot 2C_6H_4Br_2$[1a] and $[Cd(NO_3)_2(L)_2]$ (L = *N*,*N*-bis(2-pyridyl)(4-pyridylmethyl)amine),[17a] where the Cd(II) centers lie in similar distorted octahedral environments.

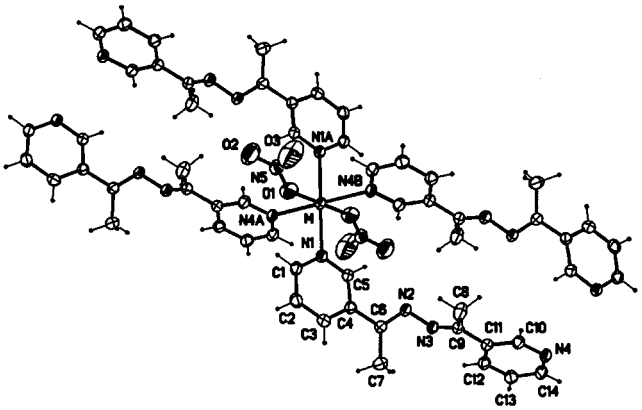

Figure 5. $\{MN_4O_2\}$ coordination environment at the metal centers of **3** (M = Cd) and **4** (M = Co), drawn with 30% probability ellipsoids. The metal atom resides on a crystallographic inversion center.

The $\{CoN_4O_2\}$ coordination sphere of the Co(II) center in **4** is unusual. To our knowledge, all Co(II) centers in coordination polymers generated from cobalt nitrate and N,N′-bidentate ligands adopt a $\{CoN_3O_4\}$[10c−g,14b] coordination environment. Compound **4** reported herein represents the first example of a $\{CoN_4O_2\}$ coordination sphere in coordination polymers. One of the Co−N bond lengths is 2.147(2) Å, which is significantly shorter than the corresponding Co−N bond distances (2.210(2)−2.261(2) Å) in the $\{CoN_4N'_2\}$ coordination spheres found in $[Co(pyrimidine)_2(NCS)_2)]$,[9e] $[Co(pyrazine)_2(NCS)_2)]$,[9e,10a] $[Co(4,4'\text{-trimethylenebipyridine})_2(NCS)_2]$, and $[Co(L1)_2(NCS)_2]$[14f] but is consistent with the Co−N bond distances in a $\{CoN_3O_4\}$ coordination sphere.[10c−g,14b] Compared to those of L1, the two 3-pyridyl donor groups in each L2 ligand in both **3** and **4** are not planar but are rotated by 90° with respect to one another. This is likely due to a combination of (a) the steric influence of the methyl groups attached to the −(Me)C=N−N=C(Me)− spacer as the compound assembles in the solid state and (b) the necessity of the ligand to depart from the planar transoid conformation adopted in **1** and **2** in order to link the cobalt or cadmium centers in a linear chain fashion (see below).

2. Polymeric Structures. (a) Of 1 and 2. In the solid state, compound **1** adopts a novel infinite two-dimensional interpenetrating brick wall pattern that extends in the crystallographic *bc* plane. Figure 6 shows a view perpendicular to these layers. Each quasi-rectangular brick unit consists of six Cd(II) metal centers and six L1 ligands, creating a large 66-membered-ring structure with a (crystallographic) cross-sectional area of ca. 27.52 × 13.04 Å^2. Unfortunately, the full potential for porosity is precluded by 2-fold interpenetration. Interpenetration of

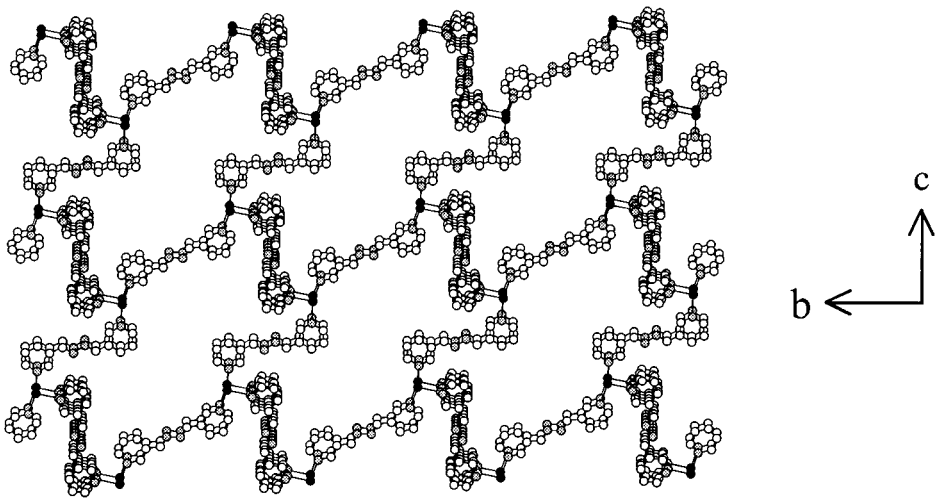

Figure 6. Molecular brick wall motif constructed from the distorted T-joint building blocks of **1** (viewed down the crystallographic *a* axis). Cadmium centers are shown as black circles, nitrogen atoms, as gray circles, and carbon atoms, as open circles. The NO_3^- ions and the hydrogen atoms are omitted for clarity.

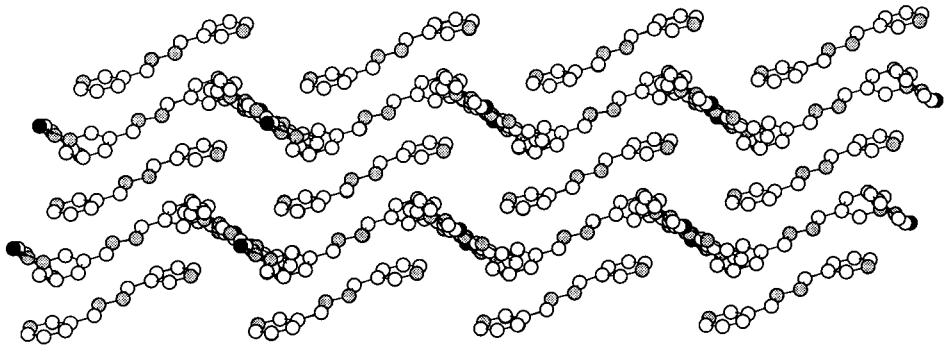

Figure 7. View down the *c* axis of **1**, showing the $\pi-\pi$ stacking system generated from face-to-face alternating stacking of coordinated and uncoordinated L1 ligands. Cadmium centers are shown as black circles, nitrogen atoms, as gray circles, and carbon atoms, as open circles. The NO_3^- ions and the hydrogen atoms are omitted for clarity.

polymeric frameworks within a crystal is a common phenomenon in many polymeric structures.[18] In principle, longer organic spacers and larger void spaces within the structure may result in a higher degree of interpenetration. This principle has been well demonstrated by a series of adamantoid systems.[19] On the other hand, the ability of $\pi-\pi$ interactions to promote more efficient packing between adjacent lattices may decrease the degree of interpenetration. This is a possible explanation for the decrease in the number of interwoven lattices from the three interlocked brick wall sheets in $[Cd(dpb\text{-}F_4)_{1.5}(NO_3)]$[20] to two in compound **1**.

The two-dimensional brick wall layers in **1** are not flat but undulate due to the orientations of the N-donors on the pyridyl rings and due to the zigzag −CH═N−N═CH− bridge between the two terminal 3-pyridyl groups. There are three different Cd···Cd distances in each brick unit: 13.01(4), 14.57(4), 13.04(3) Å. The most important feature in **1** is that there is 0.5 (per formula) uncoordinated, crystallographically independent L1 spacers located between the two-dimensional nets. The uncoordinated L1 spacers stack with two of the six coordinated L1 ligands in a face-to-face fashion via weak noncovalent $\pi-\pi$ interactions[21] ($d_{\pi-\pi} = 3.70$ Å) along the crystallographic *a* axis (perpendicular to the layers; see Figure 7). Even such weak $\pi-\pi$ interactions, however, serve as important driving forces to cross-link the two-dimensional sheets into a novel three-dimensional network with infinite channels running along the crystallographic *a* axis (Figure 6). The interlayer Cd···Cd distance is 7.40 Å. The participation of bidentate organic spacers such as 4,4′-bipyridine and 1,2-bis(4-pyridyl)ethane in the formation of polymeric frameworks by both coordination and hydrogen-bonding interactions is common.[22,23] Sometimes, weak hydrogen-bonding connectors are effective in extending the dimensions of the network.[24] A few examples have shown that the organic ligands involved (presumably) in the nucleation process use both coordination and $\pi-\pi$ interactions to construct the framework, but in all previous cases, free (uncoordinated) organic ligands have not been involved.[25] In compound **1**, the free L1 organic spacers do play a critical role in the formation of a $\pi-\pi$ stacking

(18) Batten, S. C.; Robson, R. *Angew. Chem., Int. Ed. Engl.* **1998**, *37*, 1460.
(19) (a) MacGillvary, L. R.; Subramanian, S.; Zaworotko, M. J. *J. Chem. Soc., Chem. Commun.* **1994**, 1325. (b) Blake, A. J.; Champness, N. R.; Chung, S. S.; Li, W.-S.; Schröder, M. *Chem. Commun.* **1997**, 1005. (c) Carlucci, L.; Ciani, G.; Proserpio, D. M.; Sironi, A. *J. Chem. Soc., Chem. Commun.* **1994**, 2755.
(20) Fujita, M.; Kwon,Y. J.; Sasaki, O.; Yamaguchi, K.; Ogura, K. *J. Am. Chem. Soc.* **1995**, *117*, 7287.
(21) Desiraju, G. R.; Gavezzotti, A. *Acta Crystallogr.* **1989**, *B45*, 473.
(22) (a) Sharma, C. V. K.; Rogers, R. D. *Chem. Commun.* **1998**, 1083. (b) Goodgame, D. M. L.; Menzer, S.; Smith, A. M.; Williams, D. J. *Chem. Commun.* **1997**, 339.
(23) (a) Munno, G. D.; Armentano, D.; Poerio, T.; Julve, M.; Real, J. A. *J. Chem. Soc., Dalton Trans.* **1999**, 1813. (b) Moliner, N.; Real, J. A.; Munoz, M. C.; Martinez-Manez, R.; Juan, J. M. C. *J. Chem. Soc., Dalton Trans.* **1999**, 1375.
(24) Carlucci, L.; Ciani, G.; Proserpio, D. M.; Sironi, A. *J. Chem. Soc., Dalton Trans.* **1997**, 1801.
(25) (a) Yaghi, O. M.; Li, H.; Groy, T. L. *Inorg. Chem.* **1997**, *36*, 4292. (b) Blake, A. J.; Champness, N. R.; Khlobystov, A. N.; Lemenovski, D. A.; Li, W.-S.; Schröder, M. *Chem. Commun.* **1997**, 1339.

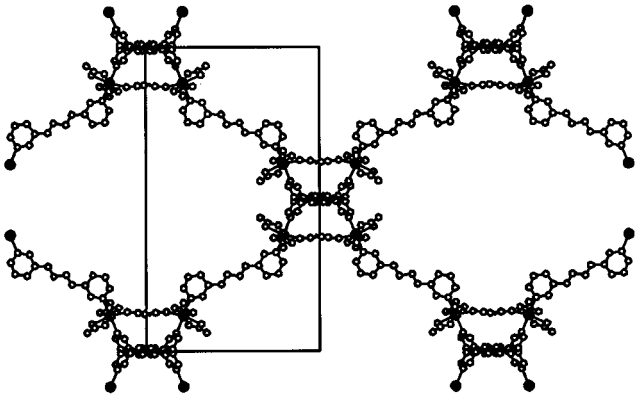

Figure 8. Linking of the distorted "F-joint" units in **2**, showing Co−L2 "column" fragments, formed from two of the three independent L1 ligands and the Co atoms, and the linking ligands which produce the three-dimensional framework. The view is down the *c* axis. Cobalt centers are shown as larger black circles.

system and, moreover, serve as the agents that allow $\pi-\pi$ interactions to expand the dimensionality of **1** from 2 to 3.

A really unexpected and remarkable polymeric pattern is found in **2**, based on the linking together of the distorted $Co(L1)_{1.5}$ "F-joints" described above. Figure 8 shows a fragment of one of the four crystallographically equivalent interpenetrating polymeric networks present in **2**, illustrating how the F-joint units are conjoined. The unit cell is shown for comparison with Figures 9 and 10. Of the three independent L2 ligands coordinated to each Co(II) center, two extend in a zigzag fashion approximately along the crystallographic *c* axis (roughly into the paper in Figure 8). The connectivity between these two L2 ligands and the cobalt atoms gives rise to Co−L2 "columns" running along the *c* axis. These (conceptual) columns are connected together in the crystallographic *ab* plane (the view in Figure 8 is perpendicular to this plane) by the third L2 ligand. The large oval spaces indicated in Figure 8 are occupied by the Co−L2 column part of the second of the four crystallographically equivalent frameworks, via a simple translation along the crystallographic *a* axis (horizontal in Figure 8) of the framework shown in Figure 8, by a distance of one *a* axis length. Figure 9 shows the three-dimensional network generated from these two frameworks. Again, the (smaller) voids appearing in Figure 9 are not empty but are occupied by the Co−L2 "column" parts of the remaining two crystallographically equivalent frameworks. These four frameworks interweave to give the full 4-fold-level interpenetrating complex three-dimensional structure, which is shown in Figure 10 (the view is down the *c* axis again). In common with many two- or three-dimensional coordination polymers, the potential for void space is severely reduced by interpenetration. Nonetheless, small voids still exist in **2**, in which a disordered water molecule is located. So far, a number of organic/inorganic coordination polymers with the metal/ligand composition $M(L)_{1.5}$ (L = ligand) have been reported, exhibiting versatile polymeric motifs such as molecular ladder,[9d,10d,14a] brick wall,[18] molecular bilayer,[10c] 3D-framework,[26] molecular parquet,[14b,27] and zigzag chain motifs.[14a] The structure of **2** reported herein is, to the best of our knowledge, unprecedented and is a new polymeric pattern generated from the general $M(L)_{1.5}$ composition.

(b) Of 3 and 4. In the solid state, compound **3** adopts a chain motif, with the Cd(II) centers linked together via four crystallographically equivalent L2 ligands into an undulating one-dimensional chain running along the crystallographic [101] direction. Two adjacent chains are shown in Figure 11. The individual "links" in the chains consist of $M_2(L2)_2$ units, which can be viewed as 22-membered rings enclosed by two Cd(II) atoms and two L2 ligands. The approximate (crystallographic) dimensions of the rings are 12×5 Å^2. The intrachain Cd···Cd separation is 12.73(4) Å. Two crystallographically equivalent monodentate NO_3^- ions are located above and below the $M_2(L2)_2$ ring planes. In addition, interchain hydrogen-bonding interactions are present in **3**, involving the uncoordinated O(2) of the monodentate nitrate ion and H(1) on the 3-pyridyl group of an L2 ligand in an adjacent chain. The O(2)···H(1) contact is 2.67(4) Å. The O(2)···C(1) distance and O(2)···H(1)−C(1) angle are 3.40(4) Å and 135.33(5)°, respectively (Figure 11). The existence and structural importance of weak C−H···O hydrogen-bonding interactions are now well established[28] and are present in many molecular and polymeric compounds, such as $(C_{14}H_{12}N_2)[Cu(opba)_2]\cdot 3H_2O$, $Na_2(C_{12}H_{12}N_2)$-$[Cu(opba)_2]\cdot 4H_2O$ (opba = *o*-phenylenebis(oxamate)),[29] and [Ag(pyrimidine)(NO_3)].[30] O···H−C hydrogen bonds, although weak, contribute significantly to the structural organization of **3** in the crystalline phase, giving rise to a two-dimensional arrangement in which one-dimensional chains align together in a face-to-face fashion to generate elliptical channels traveling along the crystallographic direction. The packing diagram in Figure 12 shows a view down these small channels. The interchain Cd···Cd distance is 8.58(4) Å.

Compound **4** is isostructural with **3** except that the Cd(II) centers are replaced by Co(II) atoms. The intra- and interchain Co···Co distances are 12.48(4) and 8.48(4) Å, respectively. The same interchain hydrogen-bonding system is also present in **4** (C(2)···H(1), 2.67 Å; O(2)···C(1), 3.37(4) Å; O(2)···H(1)−C(1), 132.61(5)°).

As noted above, the nonplanarity of the individual L2 ligands in **3** and **4** is necessary to generate the linear arrangement of metal centers in these two compounds. A planar transoid conformation of the pyridyl rings such as that found in **1** and **2** would orient the pyridyl rings in two different directions and would not allow them to converge at the neighboring metal center in the linear chain. Of course, it is still not clear why the L2 ligands do not remain planar and simply adopt another structure, such as a higher dimensional framework motif, though the steric influence of the methyl groups during the self-assembly process probably plays a role.

Thermal Analysis. Compounds **1** and **2** were heated to 650 °C and **3** and **4** were heated to 800 °C in an atmosphere of flowing helium. TGA measurements on compound **2** were taken after the guest water molecules were evaporated by warming the sample in air. This procedure was carried out to yield a stable predecomposition sample weight, from which an accurate weight loss could be determined. For **1**, TGA shows an initial weight loss of 32.1%, occurring from 96 to 235 °C, which corresponds to the loss of two of the four L1 ligands (calculated 32.0%). A second weight loss, corresponding to the loss of the third L1 ligand (observed 16.2%, calculated 16.0%) is found in the temperature range 237−270 °C. The last L1 ligand in **1** is released in the temperature range 272−300 °C (observed

(26) (a) Robinson, F.; Zaworotko, M. J. *J. Chem. Soc., Chem. Commun.* **1995**, 2413. (b) Power, K. N.; Hennigar, T. L.; Zaworotko, M. J. *Chem. Commun.* **1998**, 595.
(27) Doyle, G. A.; Goodgame, D. M. L.; Hill, S. P. W.; Williams, D. J. *J. Chem. Soc., Chem. Commun.* **1993**, 207.
(28) Desiraju, G. R. *Acc. Chem. Res.* **1996**, *29*, 441.
(29) Unamuno, I.; Gutiérrez-Zorrilla, J. M.; Luque, A.; Román, P.; Lezama, L.; Calvo, R.; Rojo, T. *Inorg. Chem.* **1998**, *37*, 6452.
(30) Sharma, C. V. K.; Rogers, R. D. *Cryst. Eng.* **1998**, *1*, 19.

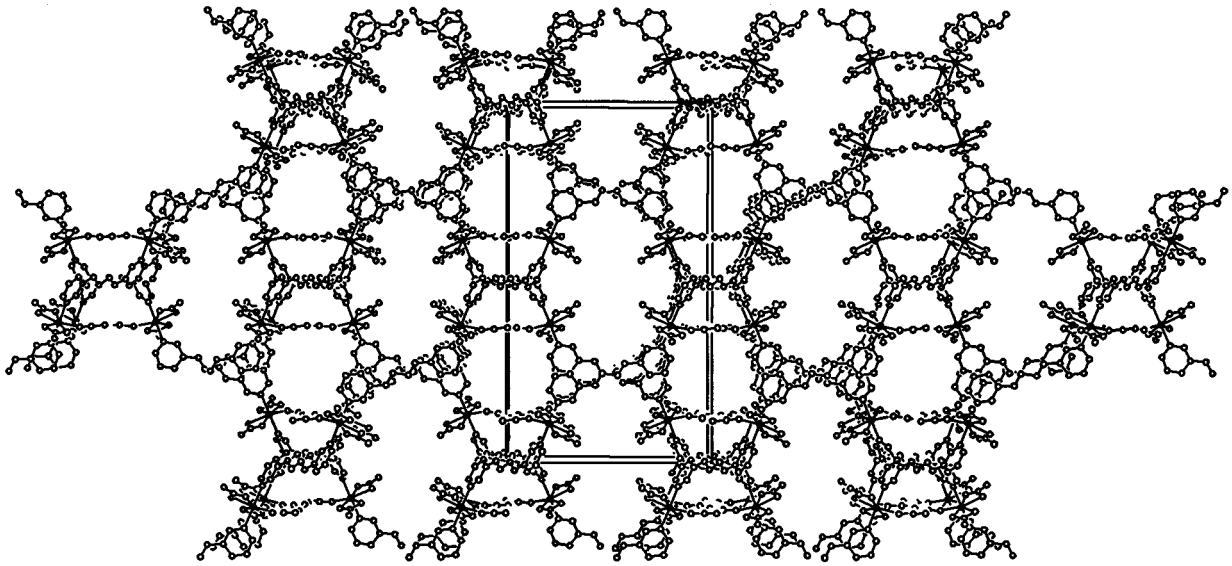

Figure 9. Perspective view of two of the four crystallographically equivalent interpenetrating 3-D frameworks in **2**, with the unit cell shown. The view is down the *c* axis, with the *a* axis horizontal.

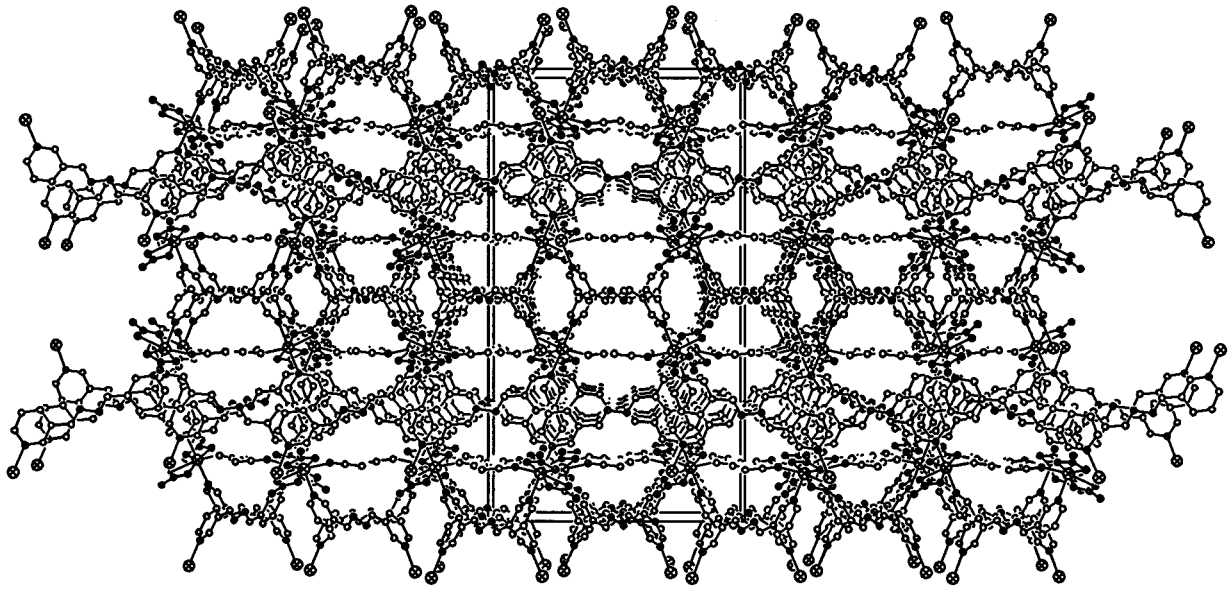

Figure 10. Perspective view of the full, three-dimensional packing diagram of **2**, formed from four equivalent interpenetrating frameworks. The orientation of the unit cell is the same as that in Figure 9.

15.7%, calculated 16.0%). A further weight loss is observed above 300 °C. This process is accompanied by the decomposition of the nitrate counterions, ultimately giving a brown, amorphous solid, which is probably CdO. The thermal decomposition behavior of compound **2** is quite different from that of **1**. The skeleton of the three-dimensional framework is stable up to 200 °C. The first weight loss of 20.2% is observed between 200 and 256 °C, which compares well with a calculated value of 20.4% for the loss of one of the three L1 ligands. This ligand loss is immediately followed by a 40.6% drastic weight loss from 257 to 267 °C, corresponding to the liberation of the remainder of the two L1 ligands (calculated 40.7%). A further weight loss is observed above 268 °C, and an uncharacterized black powder remains.

Compounds **3** and **4** have a similar thermal decomposition behavior, which is reasonable, since they possess the same polymeric motif. The TGA data for **3** show that the first weight loss, of 33.5%, occurs from 208 to 291 °C, which corresponds to the loss of two L2 ligands (calculated 33.4%). On further heating, another weight loss between 292 and 381 °C is observed, corresponding to the remaining L2 ligand (observed 17.2%, calculated 16.7%). Further weight loss is observed when **3** is heated above 400 °C, and a brown, amorphous product remains. The decomposition temperature of **4** is almost the same as that of **3**. Two L2 ligands of **4** are thermolyzed in the temperature range 207−272 °C (observed 36.2%, calculated 36.1%). A second weight loss corresponding to loss of the last L2 ligand (observed 18.1%, calculated 18.1%) is observed from 280 to 540 °C. Further weight loss occurs above 550 °C, and the final product is black and amorphous.

Conclusions

This study demonstrates that the long conjugated rigid bidentate ligands 1,4-bis(3-pyridyl)-2,3-diaza-1,3-butadiene (L1) and 2,5-bis(3-pyridyl)-3,4-diaza-2,4-hexadiene (L2) are capable of coordinating transition metal centers with both terminal 3-pyridyl nitrogen donors and of generating novel coordination polymers. The relative orientations of the nitrogen donors on

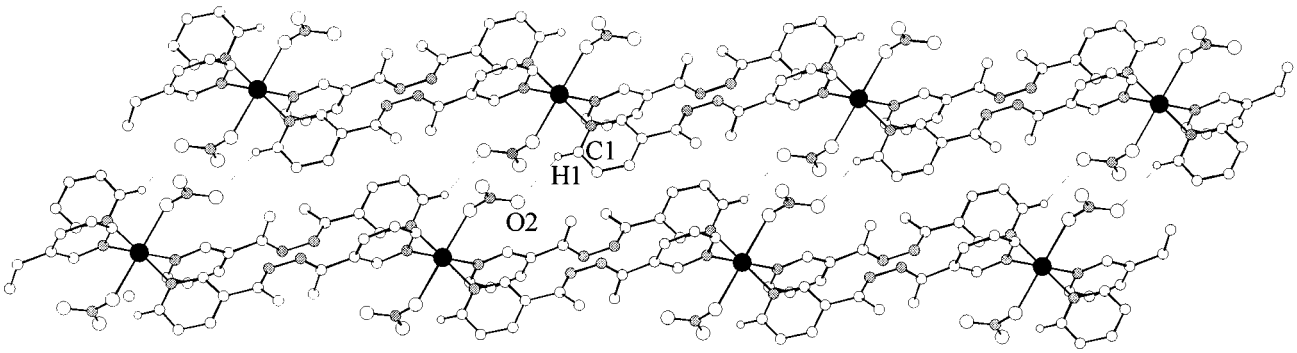

Figure 11. Adjacent one-dimensional chains in **3** and **4**, showing the O···H−C hydrogen-bonding system. Cadmium (**3**) or cobalt (**4**) centers are shown as black circles, and nitrogen atoms, as gray circles. Oxygen, carbon, and hydrogen atoms are shown as large, medium, and small open circles, respectively. Hydrogen bonds are shown as dotted lines. Hydrogen atoms except H(1) are omitted for clarity.

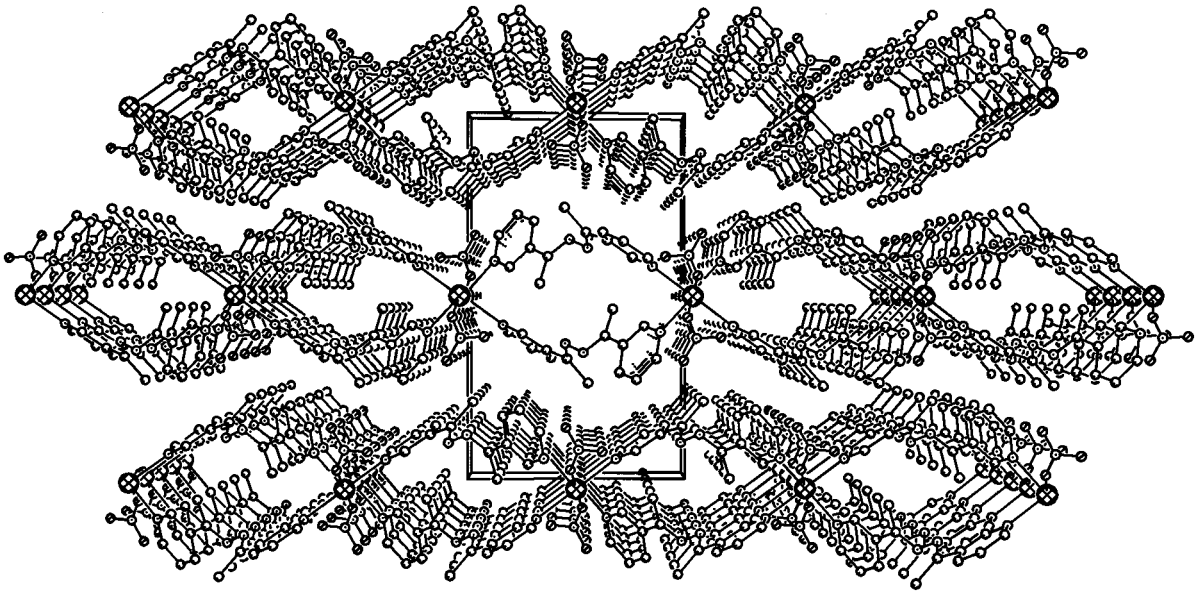

Figure 12. Perspective view down the elliptical channels in **3** and **4**, showing the alignment of the polymer strands in the solid state. The unit cell is shown; the view is down the *a* axis, with *c* horizontal. The channels are enclosed by two L2 ligands and two metal atoms. Cadmium (**3**) or cobalt (**4**) centers are shown as larger cross-hatched circles. Hydrogen atoms are omitted for clarity.

the pyridyl rings and the zigzag −CR═N−N═CR− (R = H, CH_3) spacing resulted in unusual building blocks, leading to the construction of polymeric motifs that have not been achieved using normal rigid bidentate organic ligands. Four new coordination polymers **1**−**4** were synthesized from reactions of L1 and L2 with $Cd(NO_3)_2 \cdot 4H_2O$ and $Co(NO_3)_2 \cdot 6H_2O$, respectively. The coordination geometry of the metal center plays an important role in the packing arrangement of the coordination polymer. Compounds **1** and **2** feature an $\{MN_3O_4\}$ (M = Cd, Co) heptacoordinate coordination geometry, while **3** and **4** adopt an $\{MN_4O_2\}$ (M = Cd, Co) pseudooctahedral coordination sphere. Varying R (from H to CH_3) on the −CR═N−N═CR− spacer is, for the same solvent system and metal-to-ligand ratio (1:2), a decisive factor in determining the coordination environments of the metal centers and, moreover, the topologies of the polymeric products. We are currently extending this result by preparing new Schiff-base ligands of this type with different R functional groups and with different orientations of the nitrogen donors on the pyridyl rings. We anticipate this approach to be useful for the construction of a variety of new coordination polymers with novel polymeric patterns.

Acknowledgment. Financial support was provided by the Department of Defense through Grant No. N00014-97-1-0806 and by the National Science Foundation through Grant No. DMR-9873570. We also wish to thank Dr. Richard D. Adams for the use of his single-crystal X-ray diffractometer.

Supporting Information Available: X-ray crystallographic files, in CIF format, for **1**−**4**. This material is available free of charge via the Internet at http://pubs.acs.org.

IC0006504